

# Fabrication of micro-patterned titanium dioxide nanotubes thin film and its biocompatibility

Li-jie Xiang, Chun-hui Li, Ping Yang, Jing-an Li, Nan Huang

Key Laboratory for Advanced Technologies of Materials, Ministry of Education, School of Material Science and Engineering, Southwest Jiaotong University, Chengdu 610031, People's Republic of China  
E-mail: 4828713@qq.com

Published in *The Journal of Engineering*; Received on 16th October 2014; Accepted on 20th October 2014

**Abstract:** In this study, in order to obtain a novel biomaterials surface which possesses the functions of an anticoagulant, inhibiting smooth muscle proliferation and pro-endothelialisation simultaneously, a micro-patterned titanium dioxide (TiO<sub>2</sub>)-nanotubes (P-TiO<sub>2</sub>-nanotubes) thin film was prepared on titanium (Ti) surface by photolithography combining with anodising method. The authors found that the P-TiO<sub>2</sub>-nanotubes could reduce platelet attachment and conformational change of fibrinogen (FGN) as well as promoting endothelial cells (ECs) growth compared with the TiO<sub>2</sub>-nanotubes. Notably, P-TiO<sub>2</sub>-nanotubes could significantly reduce smooth muscle cells (SMCs) proliferation compared with TiO<sub>2</sub>-nanotubes and TiO<sub>2</sub>, and the ECs and SMCs cultured on the P-TiO<sub>2</sub>-nanotubes thin film were elongated, which was suggested to be beneficial for maintaining the cell function. Therefore it is suggested that the P-TiO<sub>2</sub>-nanotubes thin film can contribute more to biocompatible functions of regulating and coordinating the behaviour of platelets, ECs and SMCs.

## 1 Introduction

Titanium dioxide (TiO<sub>2</sub>) thin film is widely applied for the surface modification of the cardiovascular implanted biomaterials due to its excellent mechanical performance and blood compatibility [1, 2]. Among the two major applied structures of TiO<sub>2</sub> crystals, anatase and rutile, rutile forms possess better blood compatibility [3] while anatase owns better cell compatibility [4]. However, the preparation of a novel TiO<sub>2</sub> thin film, which possesses both good blood compatibility and cell compatibility (to promote surface endothelialisation and inhibit hyperplasia), is still urgent for the cardiovascular implanted devices and it remains unresolved. Our previous work has demonstrated that a mixture crystal form composed of rutile and anatase can effectively inhibit platelet adhesion and enhance endothelial cells (ECs) growth simultaneously [5], but the smooth muscle cells (SMCs) involved in the hyperplasia also excessively proliferate on the TiO<sub>2</sub> thin film with mixture crystal form. To solve this problem, the surface topology, as a key factor which influences the cell behaviours, has been introduced.

Interaction of materials and cells is an important part of basic research in the field of biomaterials, wherein the material surface topology (including roughness, micro and/or nano structure) is particularly important for biological regulation of cells. The cell adhesion, proliferation and differentiation are greatly influenced by the surface topology. It has been reported by Zhong *et al.* [6] that the nanotubes with diameters ranged from 60 to 100 nm have the ability to inhibit SMCs proliferation [7]. Nevertheless, this nanotubes surface also suppresses ECs proliferation, and expresses worse blood compatibility compared with the flat surface [8]. The research of Anderson and Hinds [9] has proved that surface micro-grooves and ridges can enhance the extracellular matrix component production of the ECs, such as collagen, fibronectin (Fn) and laminin (Ln). These proteins contribute to the attachment and proliferation of the ECs, suggesting a better ECs growth of the micro-patterns. Our study also verified the speculation, demonstrating the possibility of TiO<sub>2</sub> micro-grooves and ridges improving ECs growth [5]. Thus, it is supposed that the preparation of a micro-patterned TiO<sub>2</sub>-nanotubes thin film may obtain the anticoagulation, endothelialisation and hyperplasia suppression function without additional proteins and/or biological factors introduction.

In this paper, we developed the novel micro-patterned TiO<sub>2</sub>-nanotubes thin film mentioned above on the titanium (Ti) substrate by photolithography and anodising method. A heat treatment was performed on the thin film to obtain the mixture crystal form composed of rutile and anatase, and the TiO<sub>2</sub> crystal form was detected by X-ray powder diffraction (XRD). The platelets test and fibrinogen denaturation were performed to evaluate the blood compatibility of the thin film. ECs and SMCs culture were also conducted for the investigation of the thin film on endothelialisation and hyperplasia suppression function. This micro/nano composited TiO<sub>2</sub> thin film was anticipated for application in surface physical/chemical modification of cardiovascular devices.

## 2 Experimental details

### 2.1 Fabrication of micro-patterned TiO<sub>2</sub>-nanotubes thin film

The micro-patterned TiO<sub>2</sub>-nanotubes thin film was fabricated on Ti substrate (Northwest Institute for Nonferrous Metal, China) and the process was described in Fig. 1. At the first step, the micro-patterns of grooves/ridges were prepared on the cleaned Ti foils by photolithography in advance [10]; at the second step, Ti-nanotubes were prepared on the Ti grooves of the patterned samples by the method of anodic oxidation (20 V, 2 h) [11], after the remaining photoresist was removed as above, the Ti-nanotubes/Ti micro-strips were obtained (labelled as P-Ti-nanotubes). The flat Ti foils with nanotubes (labelled as Ti-nanotubes) and Ti foils were fabricated as a control. All the samples were heat treated at 500°C for 1 h (in air, 1 standard atmosphere), and the samples were labelled as P-TiO<sub>2</sub>-nanotubes, TiO<sub>2</sub>-nanotubes and TiO<sub>2</sub>.

### 2.2 Characterisation of the micro-patterned TiO<sub>2</sub>-nanotubes thin film

The surface topographies of P-TiO<sub>2</sub>-nanotubes, TiO<sub>2</sub>-nanotubes and TiO<sub>2</sub> were characterised using scanning electron microscopy (SEM, JSM-7001F, Japan) [12]. Surface wettabilities of the P-TiO<sub>2</sub>-nanotubes, TiO<sub>2</sub>-nanotubes and TiO<sub>2</sub> samples were determined by measuring the water contact angle [13]. The crystal structure of the TiO<sub>2</sub> was identified by X-ray diffraction (XRD, X' Pert ProMPD) [14].

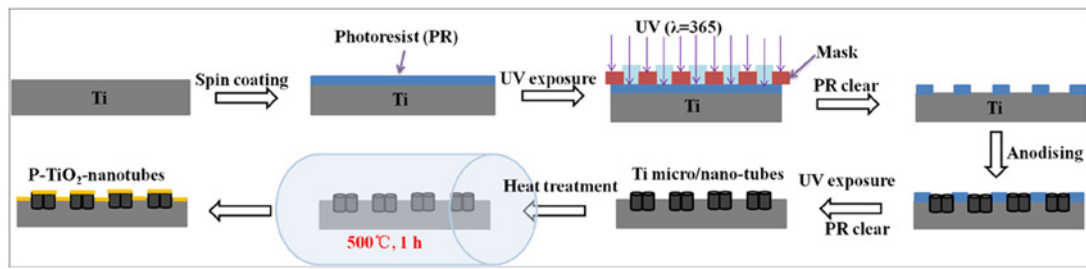


Fig. 1 Sketch map of the preparation of P-TiO<sub>2</sub>-nanotubes on Ti substrate. 92 × 21 mm (300 × 300 DPI)

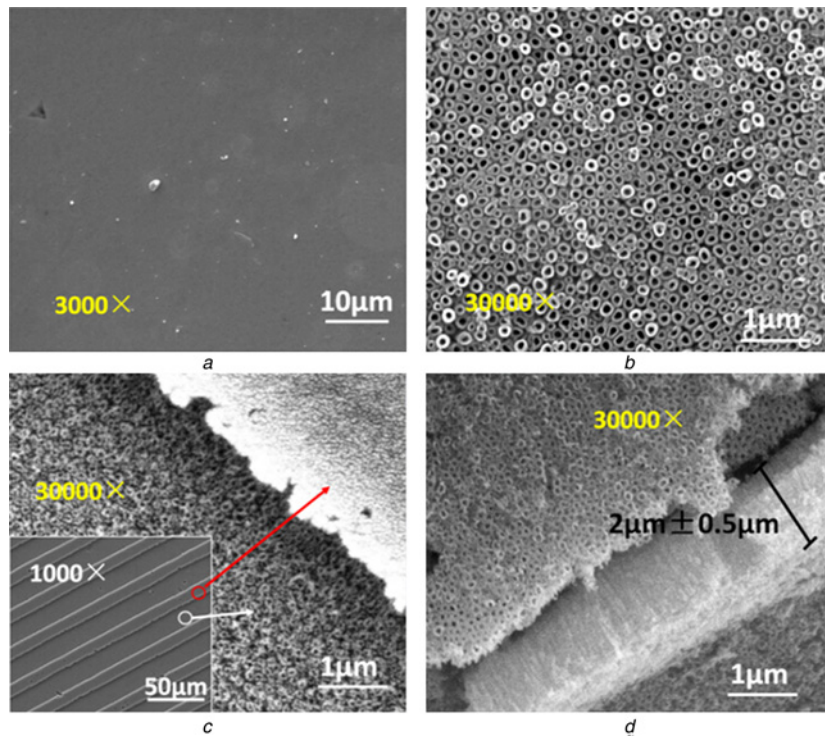


Fig. 2 SEM images of the morphology of

- a TiO<sub>2</sub>
- b TiO<sub>2</sub>-nanotubes
- c P-TiO<sub>2</sub>-nanotubes
- d Thickness of the nanotubes.

(SEM: scanning electron microscopy). 280 × 240 mm (66 × 66 dots per inch (DPI))

### 2.3 Blood compatibility of the micro-patterned TiO<sub>2</sub>-nanotubes thin film

Platelet adhesion test and conformational change of fibrinogen was performed as the previous work [15, 16]. The fluorescence images and statistical counting of attached platelets and the denatured fibrinogen were obtained to evaluate the blood compatibility.

### 2.4 Cell compatibility of the micro-patterned TiO<sub>2</sub>-nanotubes thin film

ECs were derived and cultured by a typical method that has been widely reported [17], and the third generation of the cells was used for the surface endothelialisation evaluation (density: 5 × 10<sup>4</sup> cells/ml, standard culture condition for 1, 3 and 5 days). The morphology of ECs in samples was observed under a fluorescence microscope (OLIMPUS-IX51, Japan) after staining. ECs numbers in the samples were detected using CCK-8 assay [18]. ECs morphology indexes including major/minor, orientation angle and spreading area were examined according to our previous work [12].

SMCs were obtained and cultured using a tissue explants adherent method [19], and the third generation of the cells were used for

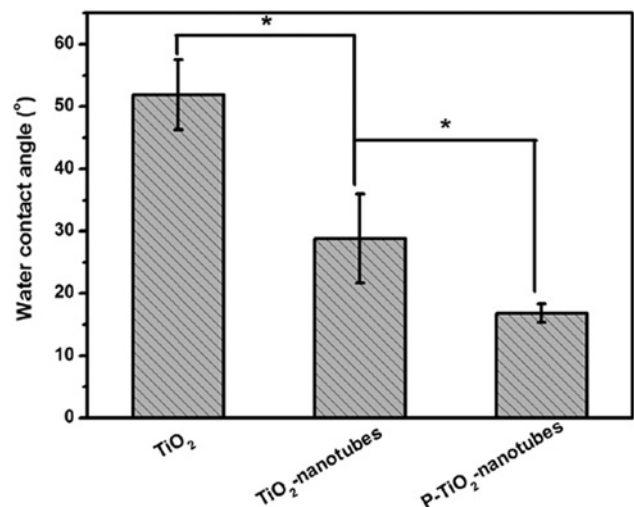
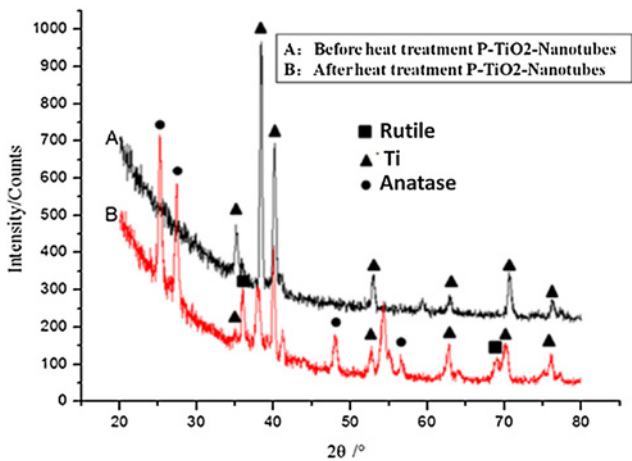


Fig. 3 Detection of wettability of: TiO<sub>2</sub>, TiO<sub>2</sub>-nanotubes and P-TiO<sub>2</sub>-nanotubes  
\**p* < 0.05, mean ± SD and *N* = 3. 55 × 39 mm (300 × 300 DPI)



**Fig. 4** Characterisation of XRD of:  $\text{TiO}_2$  films on P- $\text{TiO}_2$ -nanotubes before and after heat treatment  
XRD: X-ray diffraction. 342 × 240 mm (64 × 64 DPI)

the anti-hyperplasia evaluation (density:  $5 \times 10^4$  cells/ml, standard culture condition for 1 and 3 days). After the 4% paraformaldehyde fix step and the rinse operation, rhodamine staining was performed for the SMC morphology observation. SMCs attachment and proliferation in the samples were investigated using CCK-8 assay.

### 2.5 Statistical analysis

In this paper, all the quantitative results were reported as mean ± standard deviation (SD). The data were analysed by the software SPSS 11.5 (Chicago, IL). Statistical significance was accepted at

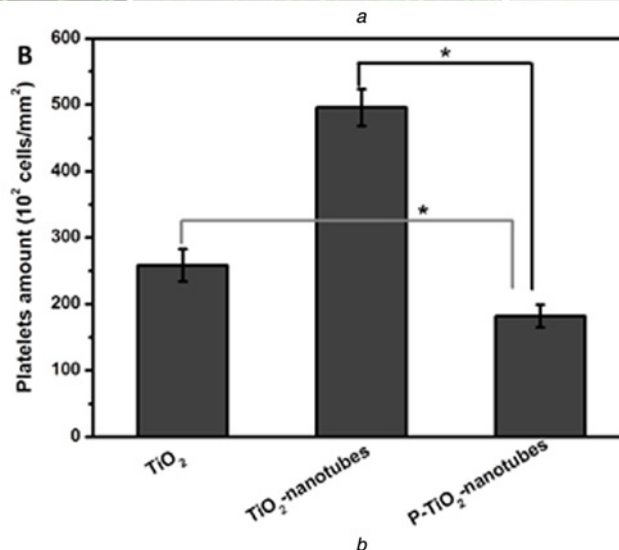
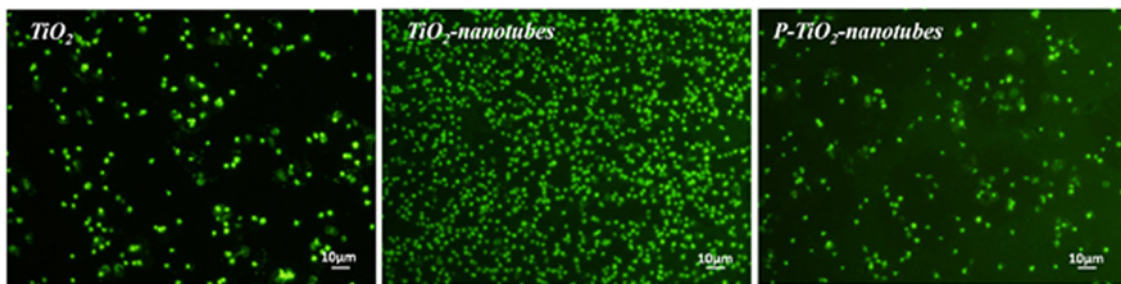


**Fig. 5** Blood compatibility of the micro-patterned  $\text{TiO}_2$ -nanotubes thin film

a Platelet adhesion fluorescence microscope images of  $\text{TiO}_2$ ,  $\text{TiO}_2$ -nanotubes and P- $\text{TiO}_2$ -nanotubes

b Amount of adherent platelets on various sample surfaces after incubation with platelet-rich-plasma for 1 h. The samples included the  $\text{TiO}_2$ ,  $\text{TiO}_2$ -nanotubes and P- $\text{TiO}_2$ -nanotubes (\* $p < 0.05$ , mean ± SD and  $N = 3$ ). 50 × 35 mm (300 × 300 DPI)

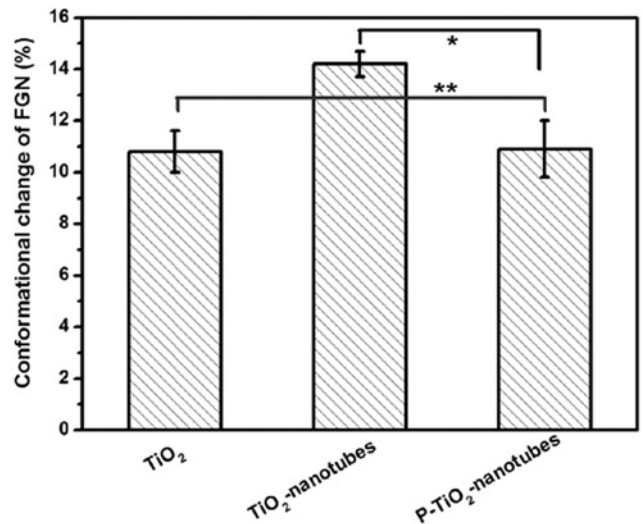


**Fig. 6** Conformational change of fibrinogen on the  $\text{TiO}_2$ ,  $\text{TiO}_2$ -nanotubes and P- $\text{TiO}_2$ -nanotubes samples  
\* $p < 0.05$ , mean ± SD and  $N = 4$ . 55 × 39 mm (300 × 300 DPI)

the  $p$ -value  $< 0.05$  ( $p < 0.05$ ). 3–5 parallel samples were set in each characterisation.

## 3 Results and discussion

### 3.1 Characterisation of the micro-patterned $\text{TiO}_2$ -nanotubes thin film

Fig. 2 shows the SEM images of the  $\text{TiO}_2$ ,  $\text{TiO}_2$ -nanotubes and P- $\text{TiO}_2$ -nanotubes thin films.  $\text{TiO}_2$  (Fig. 2a) displayed a smooth

surface while TiO<sub>2</sub>-nanotubes thin films (Fig. 2b) exhibited homogeneous nanotubes with the 80–100 nm diameters. It could be seen from the P-TiO<sub>2</sub>-nanotubes thin films (Fig. 2c) that the nanotubes (diameter ranging from 80 to 100 nm) distributed in the micro-grooves, and the smooth surface distributed on the micro-ridges. The thickness of the nanotubes was about 2.0 ± 0.5 μm (Fig. 2d).

Fig. 3 presents the water contact angle measurements of the TiO<sub>2</sub>, TiO<sub>2</sub>-nanotubes and P-TiO<sub>2</sub>-nanotubes thin films. Obviously, the water contact angle of the P-TiO<sub>2</sub>-nanotubes thin film was significantly less than the TiO<sub>2</sub>-nanotubes and TiO<sub>2</sub> (P-TiO<sub>2</sub>-nanotubes

<TiO<sub>2</sub>-nanotubes < TiO<sub>2</sub>, \**p* < 0.05), suggesting the hydrophilicity tendency as: P-TiO<sub>2</sub>-nanotubes > TiO<sub>2</sub>-nanotubes > TiO<sub>2</sub>, which indicated that P-TiO<sub>2</sub>-nanotubes thin film was more conducive to protein adhesion and further cell proliferation.

Fig. 4 shows the XRD results of P-TiO<sub>2</sub>-nanotubes thin films before and after heat treatment. Before heat treatment (Fig. 4a), the P-TiO<sub>2</sub>-nanotubes thin film was composed of neither rutile phase nor anatase phase. After heat treatment (Fig. 4b), the P-TiO<sub>2</sub>-nanotubes thin film was composed of rutile and anatase phase, taking into account the blood compatibility and cell

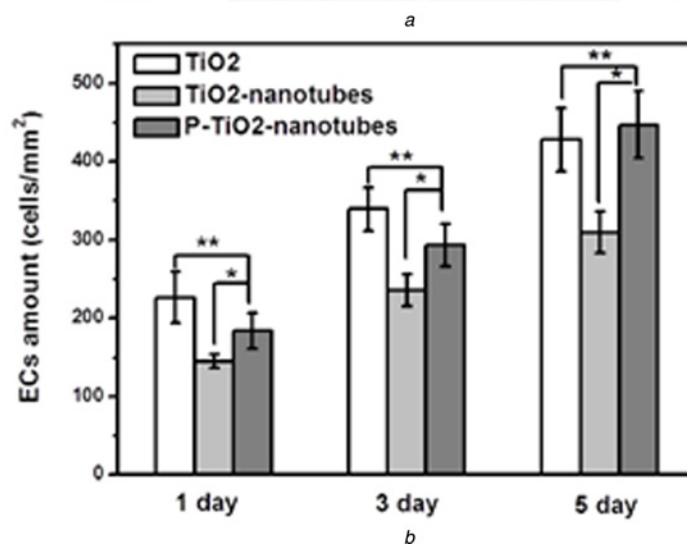
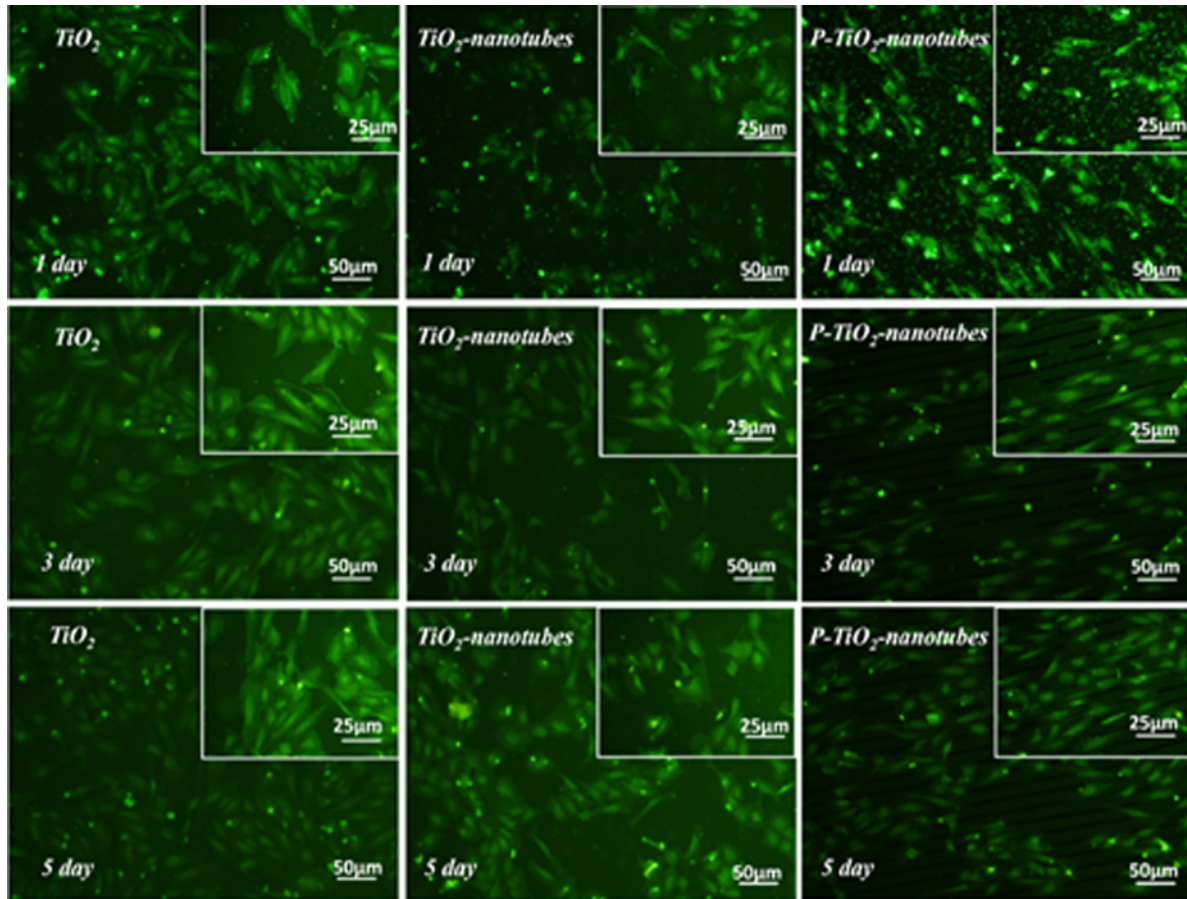
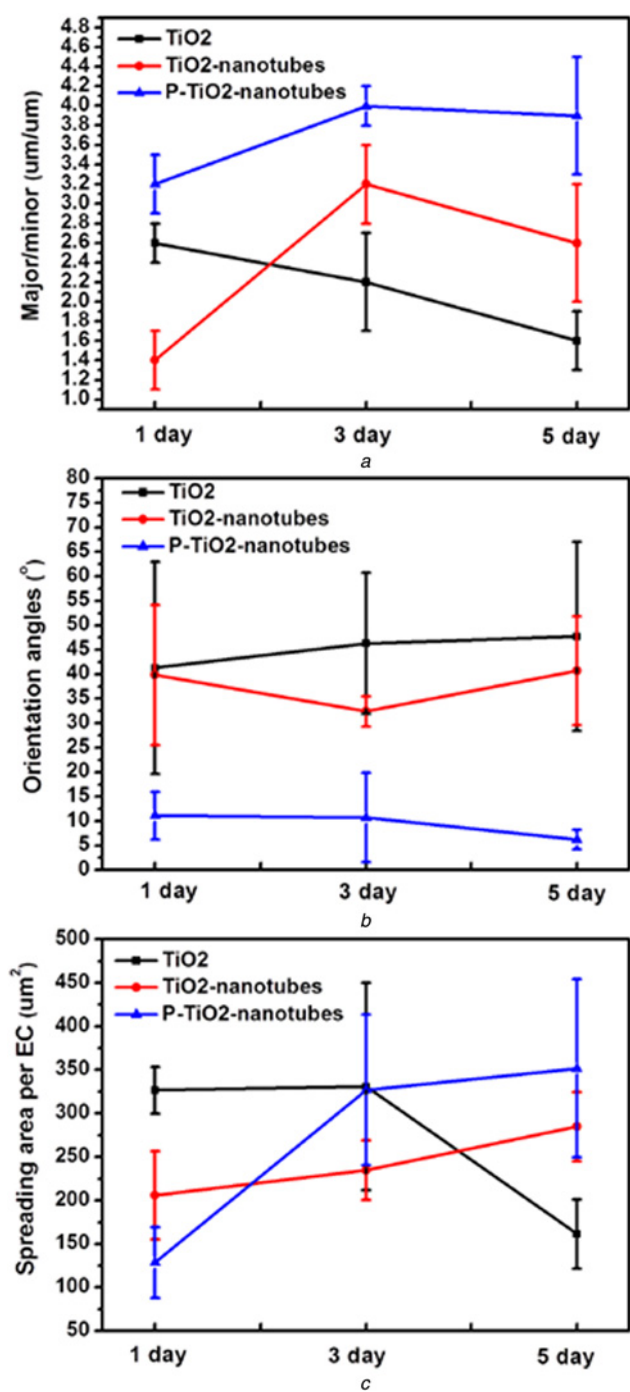


Fig. 7 Cell compatibility of the micro-patterned TiO<sub>2</sub>-nanotubes thin film

a Immunofluorescence staining micrographs of ECs after cultured on TiO<sub>2</sub>, TiO<sub>2</sub>-nanotubes and P-TiO<sub>2</sub>-nanotubes for 1, 3 and 5 day, respectively

b ECs attachment and proliferation on TiO<sub>2</sub>, TiO<sub>2</sub>-nanotubes and P-TiO<sub>2</sub>-nanotubes using CCK-8 assay. (\**p* < 0.05, \*\**p* > 0.05, mean ± SD and *N* = 3). 41 × 50 mm (300 × 300 DPI)



**Fig. 8** Calculation of the morphology index of ECs  
 a Major/minor  
 b Orientation angle  
 c Spreading area ( $N = 15$ , mean  $\pm$  SD and  $*p < 0.05$ )  $34 \times 66$  mm ( $300 \times 300$  DPI)

compatibility, because the anatase phase was proved to have better cell compatibility.

### 3.2 Blood compatibility of the micro-patterned TiO<sub>2</sub>-nanotubes thin film

The fluorescence images of the adherent platelets on the P-TiO<sub>2</sub>-nanotubes thin film are shown in Fig. 5a. It could be seen that the TiO<sub>2</sub>-nanotubes and TiO<sub>2</sub> samples showed more platelets than the P-TiO<sub>2</sub>-nanotubes sample, and the platelets statistical calculation result (Fig. 5b) also proved the phenomenon (platelets

number: P-TiO<sub>2</sub>-nanotubes < TiO<sub>2</sub> < TiO<sub>2</sub>-nanotubes). The platelets test results indicated that the P-TiO<sub>2</sub>-nanotubes thin film possessed better blood compatibility.

The conformational change of fibrinogen, that is, exposure of  $\gamma$  chain, could reveal the thrombosis tendency [20]. Fig. 6 displayed the conformational changes of fibrinogen detected from the TiO<sub>2</sub>, TiO<sub>2</sub>-nanotubes and P-TiO<sub>2</sub>-nanotubes thin film. The P-TiO<sub>2</sub>-nanotubes thin film showed significantly lower absorbance compared with the TiO<sub>2</sub>-nanotubes, but no significantly different absorbance to the TiO<sub>2</sub> thin film. The result indicated that the P-TiO<sub>2</sub>-nanotubes and TiO<sub>2</sub> thin film possessed better blood compatibility compared with TiO<sub>2</sub>-nanotubes, and this result was consistent with the platelet adhesion result.

### 3.3 Cell compatibility of the micro-patterned TiO<sub>2</sub>-nanotubes thin film

Fig. 7 shows the EC immunofluorescence images and the statistical results of EC number on the P-TiO<sub>2</sub>-nanotubes, TiO<sub>2</sub>-nanotubes and TiO<sub>2</sub>. It could be seen from the EC immunofluorescence images (Fig. 7a) that the morphology of EC on the P-TiO<sub>2</sub>-nanotubes thin film was affected by the micro-grooves and ridges. The ECs on the P-TiO<sub>2</sub>-nanotubes thin film grew along the micro-grooves and ridges and showed bionic elongated morphology, whereas the ECs on the TiO<sub>2</sub>-nanotubes and TiO<sub>2</sub> samples distributed in random orientations and showed elliptic, rounded or polygonal morphology. Thus, the P-TiO<sub>2</sub>-nanotubes thin film was considered to be helpful for the formation of the bionic microenvironment. On the other hand, the EC numbers on the P-TiO<sub>2</sub>-nanotubes and TiO<sub>2</sub> were significantly greater than the value on the TiO<sub>2</sub>-nanotubes. It has been reported that the nanotubes with the 100 nm diameter have the effect of inhibiting cell attachment and proliferation, and this fact may explain the few ECs on the TiO<sub>2</sub>-nanotubes. The micro-grooves and ridges could elongate the ECs morphology, and this cell phenotype has better cell proliferation ability [21, 22], and it could reverse the cell inhibiting effect caused by TiO<sub>2</sub>-nanotubes.

Fig. 8 exhibits the EC morphology index including major/minor, orientation angle and spreading area. The major/minor index of ECs (Fig. 8a) on P-TiO<sub>2</sub>-nanotubes thin film was significantly higher than the parameters of TiO<sub>2</sub>-nanotubes and TiO<sub>2</sub>, suggesting elongated cell morphology compared with the two references, which were consistent with the EC immunofluorescence images. Notably, the major/minor index of ECs was proved positively correlated to the anti-coagulation factor release of ECs, such as NO and PGI<sub>2</sub> [12], which meant better anti-coagulation of the ECs. The orientation angle index of ECs (Fig. 8b) on P-TiO<sub>2</sub>-nanotubes thin film was significantly lower than the parameters of TiO<sub>2</sub>-nanotubes and TiO<sub>2</sub>, indicating the parallel orientation between cell and cell which was regulated by the micro-grooves and ridges, and the orientation angle of ECs on P-TiO<sub>2</sub>-nanotubes thin film even reduced within 10° after 5 days culture. The ECs with parallel orientation usually survive in vivo, caused by the blood flow shear stress, which was conducive to the normal function of the ECs. From the cell spreading statistical results (Fig. 8c), no remarkable difference existed between the ECs on P-TiO<sub>2</sub>-nanotubes, TiO<sub>2</sub>-nanotubes and TiO<sub>2</sub>. That meant the thin film topology had no effects on the EC spreading.

Fig. 9 shows the SMC immunofluorescence images and the statistical results of SMC number on the P-TiO<sub>2</sub>-nanotubes, TiO<sub>2</sub>-nanotubes and TiO<sub>2</sub>. Both the immunofluorescence images and the cell statistical results presented a significant effect of P-TiO<sub>2</sub>-nanotubes in inhibiting SMC adhesion and proliferation compared with TiO<sub>2</sub>-nanotubes and TiO<sub>2</sub> (SMC number: P-TiO<sub>2</sub>-nanotubes < TiO<sub>2</sub>-nanotubes < TiO<sub>2</sub>). As mentioned above, nanotubes with the 100 nm diameter have the effect of inhibiting cell adhesion and proliferation, and that is the reason why SMC numbers on P-TiO<sub>2</sub>-nanotubes and TiO<sub>2</sub>-nanotubes were less than

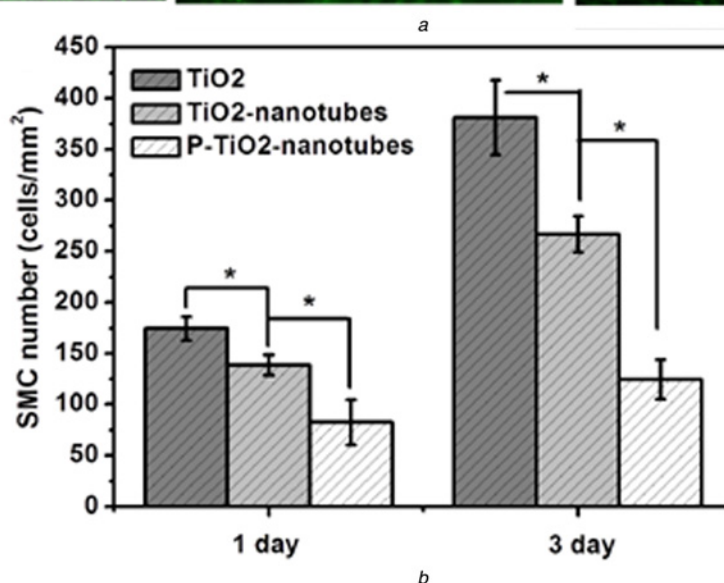
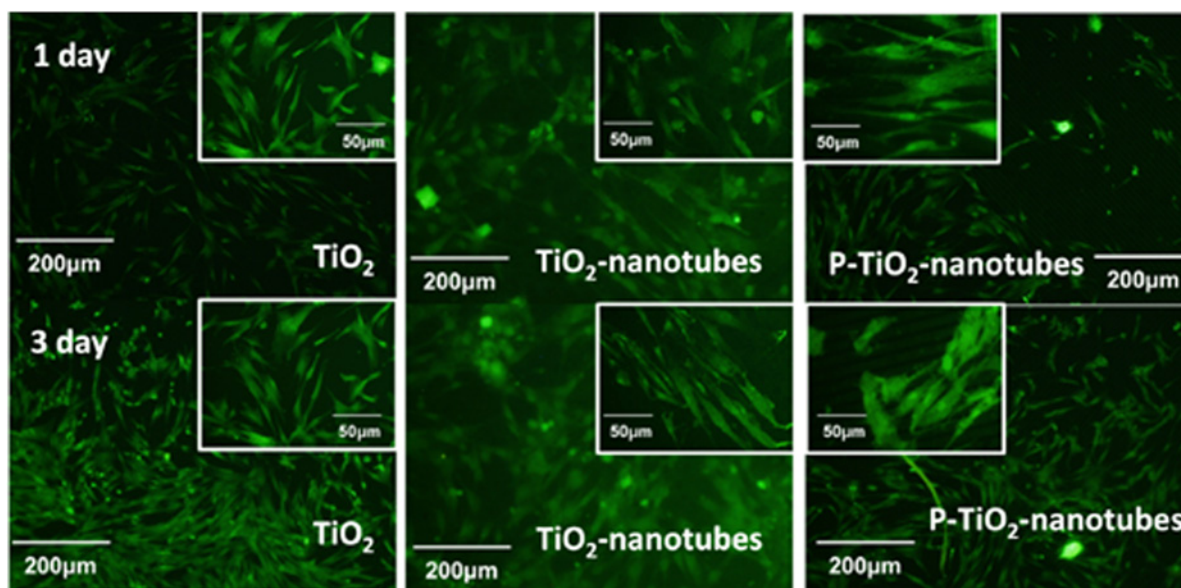


**Fig. 9** SMC immunofluorescence images and the statistical results of SMC number on the P-TiO<sub>2</sub>-nanotubes, TiO<sub>2</sub>-nanotubes and TiO<sub>2</sub>  
 a Immunofluorescence staining micrographs of SMCs after cultured on TiO<sub>2</sub>, TiO<sub>2</sub>-nanotubes and P-TiO<sub>2</sub>-nanotubes for 1 and 3 days, respectively  
 b SMCs attachment and proliferation on TiO<sub>2</sub>, TiO<sub>2</sub>-nanotubes and P-TiO<sub>2</sub>-nanotubes using CCK-8 assay. (\**p* < 0.05, mean ± SD and *N* = 3). 44 × 44 mm (300 × 300 DPI)

the values on TiO<sub>2</sub>. Our previous work proved that the micro-grooves and ridges with the width ranging from 5 to 80 µm could limit SMC to a contractile phenotype, which could inhibit the SMC itself proliferation and producing adhesion proteins [13, 17, 18].

#### 4 Conclusion

Thin films of P-TiO<sub>2</sub>-nanotubes have been prepared on the Ti substrate through photolithography and anodic oxidation. The micro/nano composited TiO<sub>2</sub> thin film possessed better blood compatibility compared with simple TiO<sub>2</sub>-nanotubes thin film and flat TiO<sub>2</sub> thin film. The P-TiO<sub>2</sub>-nanotubes thin film could also improve the human vascular ECs adhesion, proliferation and maintain the ECs physiology, morphology and function. Additionally, the P-TiO<sub>2</sub>-nanotubes thin film could effectively inhibit human vascular SMCs adhesion and proliferation. Thus, the P-TiO<sub>2</sub>-nanotubes thin film was anticipated to be potentially applied for the cardiovascular implanted biomaterials.

#### 5 Acknowledgments

The reported work has been funded by the Key Basic Research Project (no. 2011CB606204), the National Natural Science Foundation of China (no. 30870629), the Fundamental Research Funds for the Central Universities (nos. SWJTU11ZT11 and SWJTU11CX054), Postdoctoral Funds of Southwest Jiaotong University (X1101512370435 and YH1101012371444) and the China Postdoctoral Science Foundation (2014M562333).

#### 6 References

- [1] Liu J.X., Yang D.Z., Shi F., Cai Y.J.: 'Sol-gel deposited TiO<sub>2</sub> film on NiTi surgical alloy for biocompatibility improvement', *Thin Solid Films*, 2003, **429**, pp. 225–230
- [2] Abdal-hay A., Mousa H.M., Khan A., Vanegas P., Lim J.H.: 'TiO<sub>2</sub> nanorods coated onto nylon 6 nanofibers using hydrothermal treatment with improved mechanical properties', *Colloids Surf. A, Physicochem. Eng. Aspects*, 2014, **457**, pp. 275–281
- [3] Zhang X.H., Zheng X., Cheng Y., Li G.H., Chen X.P., Zheng J.H.: 'Formation of rutile fasciculate zone induced by sunlight irradiation

- at room temperature and its hemocompatibility', *Mater. Sci. Eng. C*, 2013, **33**, pp. 3289–3293
- [4] Collazos-Castro J.E., Cruz A.M., Carballo-Vila M., *ET AL.*: 'Neural cell growth on TiO<sub>2</sub> anatase nanostructured surfaces', *Thin Solid Films*, 2009, **518**, pp. 160–170
- [5] Li J.A., Yang P., Zhang K., Ren H.L., Huang N.: 'Preparation of SiO<sub>2</sub>/TiO<sub>2</sub> and TiO<sub>2</sub>/TiO<sub>2</sub> micropattern and their effects on platelet adhesion and endothelial cell regulation', *Nucl. Instrum. Methods Phys. Res. B*, 2013, **307**, pp. 575–579
- [6] Zhong S., Luo R.F., Wang X., *ET AL.*: 'Effects of polydopamine functionalized titanium dioxide nanotubes on endothelial cell and smooth muscle cell', *Colloids Surf. B, Biointerfaces*, 2014, **116**, pp. 553–560
- [7] Peng L.L., Eltgroth M.L., LaTempa T.J., Grimes C.A., Desai T.A.: 'The effect of TiO<sub>2</sub> nanotubes on endothelial function and smooth muscle proliferation', *Biomaterials*, 2009, **30**, pp. 1268–1272
- [8] Park J., Bauer S., Schmuki P., von der M.K.: 'Narrow window in nanoscale dependent activation of endothelial cell growth and differentiation on TiO<sub>2</sub> nanotube surfaces', *Nano Lett.*, 2009, **9**, pp. 3157–3164
- [9] Anderson D.E.J., Hinds M.T.: 'Extracellular matrix production and regulation in micropatterned endothelial cells', *Biochem. Biophys. Res. Commun.*, 2012, **427**, pp. 159–164
- [10] Lei L.J., Li C.H., Yang P., Huang N.: 'Photo-immobilized heparin micropatterns on Ti–O surface: preparation, characterization, and evaluation in vitro', *J. Mater. Sci.*, 2011, **46**, pp. 6772–6782
- [11] Wang Y., Wu Y.C., Qin Y.Q., *ET AL.*: 'Rapid anodic oxidation of highly ordered TiO<sub>2</sub> nanotube arrays', *J. Alloys Compd.*, 2011, **509**, pp. L157–L160
- [12] Li J.A., Zhang K., Yang P., *ET AL.*: 'Human vascular endothelial cell morphology and functional cytokine secretion influenced by different size of HA micro-pattern on titanium substrate', *Colloids Surf. B, Biointerfaces*, 2013, **110**, pp. 199–207
- [13] Li J.A., Li G.C., Zhang K., *ET AL.*: 'Co-culture of vascular endothelial cells and smooth muscle cells by hyaluronic acid micro-pattern on titanium surface', *Appl. Surf. Sci.*, 2013, **273**, pp. 24–31
- [14] Zhao Y.C., Tu Q.F., Wang J., Huang Q.J., Huang N.: 'Crystalline TiO<sub>2</sub> grafted with poly(2-methacryloyloxyethyl phosphorylcholine) via surface-initiated atom-transfer radical polymerization', *Appl. Surf. Sci.*, 2010, **257**, pp. 1596–1601
- [15] Zhou Z., Chen J., Xiang L.J., *ET AL.*: 'Fabrication of 3D TiO<sub>2</sub> micro-mesh on silicon surface and its effects on platelet adhesion', *Mater. Lett.*, 2014, **132**, pp. 149–152
- [16] Li G.C., Yang P., Qin W., Maitz M.F., Zhou S., Huang N.: 'The effect of coimmobilizing heparin and fibronectin on titanium on hemocompatibility and endothelialization', *Biomaterials*, 2011, **32**, pp. 4691–4703
- [17] Li J.A., Zhang K., Yang P., *ET AL.*: 'Research of smooth muscle cells response to fluid flow shear stress by hyaluronic acid micro-pattern on a titanium surface', *Exp. Cell Res.*, 2013, **319**, pp. 2663–2672
- [18] Li J.A., Zhang K., Xu Y., *ET AL.*: 'A novel coculture model of HUVECs and HUASMCs by hyaluronic acid micropattern on titanium surface', *J. Biomed. Mater. Res. A*, 2014, **102A**, pp. 1950–1960
- [19] Li J.A., Zhang K., Chen H.Q., *ET AL.*: 'A novel coating of type IV collagen and hyaluronic acid on stent material-titanium for promoting smooth muscle cell contractile phenotype', *Mater. Sci. Eng. C*, 2014, **38**, pp. 235–243
- [20] Li G.C., Zhang F.M., Liao Y.Z., Yang P., Huang N.: 'Coimmobilization of heparin/fibronectin mixture on titanium surfaces and their blood compatibility', *Colloids Surf. B, Biointerfaces*, 2010, **81**, pp. 255–262
- [21] Yang Z.L., Tu Q.F., Maitz M.F., Zhou S., Wang J., Huang N.: 'Direct thrombin inhibitor-bivalirudin functionalized plasma polymerized allylamine coating for improved biocompatibility of vascular devices', *Biomaterials*, 2012, **33**, pp. 7959–7971
- [22] Yang Z.L., Tu Q.F., Wang J., Huang N.: 'The role of heparin binding surfaces in the direction of endothelial and smooth muscle cell fate and re-endothelialization', *Biomaterials*, 2012, **33**, pp. 6615–6625